Highlights of Spanish Astrophysics XII, Proceedings of the XVI Scientific Meeting of the Spanish Astronomical Society held on July 15 - 19, 2024, in Granada, Spain. M. Manteiga, F. González Galindo, A. Labiano Ortega, M. Martínez González, N. Rea, M. Romero Gómez, A. Ulla Miguel, G. Yepes, C. Rodríguez López, A. Gómez García and C. Dafonte (eds.), 2025

Stellar wind impact on the early atmospheres of Earth-like planets. A MHD approximation.

Canet, A.[1,2], Varela, J.[3], and Gómez de Castro, A.I.[1,2]

[1] Joint Center for Ultraviolet Astronomy (JCUVA), Universidad Complutense de Madrid, E-28040, Madrid, Spain
[2] Facultad de Ciencias Matemáticas, S.D. Astronomía y Geodesia, Universidad Complutense de Madrid, E-28040 Madrid, Spain
[3] Institute for Fusion Studies, Department of Physics, University of Texas at Austin, Austin, TX 78712, USA

Abstract

During the early stages of their formation, sufficiently massive planets can accrete a primordial hydrogen atmosphere directly from the protoplanetary disk. The survival of these primordial atmospheres is intrinsically linked to stellar activity, with X-ray and extreme ultraviolet (XUV) radiation potentially triggering the complete photoevaporation of these envelopes, carrying significant implications for planetary habitability. While the effects of XUV radiation on primordial atmospheres of terrestrial planets have been extensively studied, the impact of stellar winds—also a byproduct of stellar activity—has not yet been explored in the context of Earth-like planets during their early evolutionary stages. In this work, an evolutionary sequence for primordial atmospheres on Earth-like planets is predicted for the first time under the influence of stellar winds from stars with varying levels of activity (rotation), spanning from 50 to 500 Myrs. Through 3D-MHD numerical simulations, this study examines how the morphology of primordial atmospheres is fundamentally dependent on stellar wind parameters, with a significant reduction in atmospheric extent observed in the case of fast-rotating stars, along with additional atmospheric erosion. This work demonstrates that a thorough characterization of stellar activity and the impact of stellar winds is essential for understanding the early atmospheres surrounding Earth-like planets. The results are also crucial for predicting and interpreting absorption features in spectral tracers of neutral hydrogen during planetary transits.

1 Introduction

In the early stages of planetary system formation, planetary cores with masses greater than 0.1 Earth masses can accrete substantial hydrogen and helium (H/He)-rich atmospheres from the protoplanetary disk. These primordial atmospheres are gravitationally bound to the planet, but their survival is heavily influenced by the planet's mass and the star's radiation. Specifically, the high-energy X-ray and extreme ultraviolet (XUV) radiation emitted by the host star can heat and expand the upper layers of these atmospheres, leading to their photoevaporation [3, 6].

Stellar rotation plays a critical role in this process. Fast-rotating stars, which tend to be magnetically active, emit higher levels of XUV radiation, leading to faster atmospheric loss, resulting in atmosphere-less rocky planets. Conversely, planets orbiting slow-rotating stars may retain a significant portion of their atmospheres throughout their entire lifetimes (e.g. [5]). This is crucial in terms of planetary habitability.

In addition to XUV radiation, stellar winds—streams of charged particles emanating from the star's corona, also contribute to atmospheric erosion [7, 8, 2]. These winds can strip away the outer layers of the atmosphere and influence its morphology by compressing or expanding the atmospheric boundary.

The aim of this study is to evaluate how stellar winds affect the evolution of early atmospheres around unmagnetized Earth-mass planets. By using 3D MHD simulations, we explored the interaction between stellar winds and photoevaporating atmospheres over time scales ranging from 50 to 500 Myr, considering both fast- and slow-rotating stars.

2 Stellar wind evolution

The properties of stellar winds depend on the rotation rate and magnetic activity of the host star, both of which evolve over time. In the present work, we obtained the activity-dependent stellar wind parameters at 1.0 au for a solar-like star (1 $M_\odot$ and 1 $R_\odot$) using the 1D axisymmetric Weber & Davis [12] solar wind model, scaled to different stellar activity levels, distinguishing between fast-rotating (active) and slow-rotating (low-activity) stars, at different stellar ages of 50, 150, 300, and 500 Myr. The WD model provides a simplified approach to predict stellar wind parameters at different distances from the stellar corona while accounting for magnetocentrifugal effects in the acceleration of stellar winds, which are particularly relevant, if not the main wind acceleration mechanism for fast-rotating stars.

The WD solutions for the propagation of stellar winds depend on the defined parameters of surface magnetic field, temperature, density, and rotation at the stellar corona. Stellar wind characteristic coronal parameters were scaled according to evolutional trends for fast- and slow-rotating stars, based on observational data for stellar rotation, surface magnetic field, and XUV luminosity for young solar-like stars [11, 10, 4] in the considered time span.

The WD model predicts faster, hotter, more magnetized, and denser winds for fast rotators, in comparison to the slow rotator case. The main parameters of the wind decrease with the stellar age as expected in both analysed cases. For each evolutionary stage, winds are super-Alfvénic, superfast magnetosonic at the fixed orbit. According to this feature, a bow shock is expected to form in front of the planetary obstacle, whose location is expected to be at further distances for lower Alfvénic Mach numbers [1].

3 MHD simulations: numerical set-up

The interaction of the stellar wind and the escaping primordial atmosphere of an Earth-like planet is studied through numerical, ideal MHD 3D simulations. We conducted our simulations in 3D spherical coordinates using the MHD module of the single-fluid PLUTO code [9], where the spatial and temporal evolution of the MHD equations of continuity, momentum, energy, and magnetic induction is performed:

$$\frac{\partial \rho}{\partial t} + \nabla \cdot (\rho \mathbf{v}) = 0 \tag{1}$$

$$\frac{\partial (\rho \mathbf{v})}{\partial t} + \nabla \cdot \left[\rho \mathbf{v}\mathbf{v} - \frac{\mathbf{B}\mathbf{B}}{4\pi} + p_T \mathbf{I} \right]^T = \rho(\mathbf{g} + \mathbf{F}_{Cor} + \mathbf{F}_{cen}) \tag{2}$$

$$\frac{\partial E_T}{\partial t} + \nabla \cdot \left[(E_T + p_T)\mathbf{v} - \frac{\mathbf{B}}{4\pi}(\mathbf{v} \cdot \mathbf{B}) \right] = \rho\left(\mathbf{g} + \mathbf{F}_{cen}\right) \cdot \mathbf{v} \tag{3}$$

$$\frac{\partial \mathbf{B}}{\partial t} + \nabla \times (\mathbf{B} \times \mathbf{v}) = 0 \tag{4}$$

The mass density, velocity, magnetic field, and gravitational acceleration (including both the acceleration due to the planetary and stellar gravity) vectors are denoted as ρ, $\mathbf{v}, \mathbf{B}$ and $\mathbf{g}$, respectively. The pressure term $p_T = p + \frac{\mathbf{B}^2}{8\pi}$ includes the corresponding thermal (p) and magnetic pressure contributions. The total energy of the system, E_T, is defined as $E_T = \rho\epsilon + \frac{\rho \mathbf{v}^2}{2} + \frac{\mathbf{B}^2}{8\pi}$, where ϵ is the internal energy per unit mass.
To take into account the effects of the orbital motion of the planet around the star, we solved the ideal MHD equations in a frame of reference co-rotating with the planet, considering a constant angular velocity $\Omega = \sqrt{GM_\star/d^3}$, where d is the orbital radius of the planet. We modified the right-hand side of the momentum and energy equations, incorporating the corresponding inertial terms of the Coriolis and centrifugal accelerations.

The spherical 3D computational grid is made of 738 points in the radial direction r, 96 for the polar angle θ, and 192 for the azimuthal angle ϕ, with $r \in [2.5, 60R_p]$, $\theta \in [0, \pi]$ and $\phi \in [0, 2\pi]$.

The stellar wind is injected from the outer boundary of the domain at $r = 60R_p$ for $\pi/2 < \phi < 3\pi/2$, fixing the stellar wind components of the magnetic field and velocity vectors, gas pressure, and density as constant boundary conditions, following the stellar wind solution obtained at each stellar age with the WD model, described in the last section.

Fixed parameters of density and temperature are defined at a spherical inner boundary of radius 2.5 R_p , to reproduce the escaping atmosphere of the planet under the influence of the XUV radiation. We modeled the evolution of the XUV-heated escaping atmosphere of a terrestrial planet orbiting a solar-like star at 1.0 au based on the atmospheric parameters (i.e. mass loss rate, atmospheric fraction, and velocity and temperature profiles) derived in the 1D hydrodynamic model of [5] for a planet with an initial atmospheric mass fraction of 0.01 planetary masses. We defined fixed values for density and temperature to match the mass-loss rates and velocity profiles and temperatures obtained in the 1D HD numerical code of [5] at each considered stellar age, both for fast and slow rotator regimens.

Initially, we run the simulations in the absence of the stellar wind, leading the planetary wind to converge to the steady state. Once the planetary wind reached stable density and velocity profiles, we launch the stellar wind from the outer boundary of the domain.

4 Results and Discussion

Our simulations reveal that the extension and morphology of planetary photoevaporating atmospheres are strongly influenced by the properties of the stellar wind and the level of stellar activity. Density distributions at the steady state for Earth-like planets in the time span between 50 and 500 Myr are shown for each model in the fast and slow-rotating stellar regimes in Fig. 1 and Fig. 2, respectively.

We found common structures in all the carried out simulations: (1) formation of a high-density region in front of the planet (light green in Fig. 1 and Fig. 2), byproduct of the compression of the atmosphere due to the action of stellar winds; (2) formation of double sonic (shocks) and alfvénic surfaces; (3) accumulation of magnetic field lines above the atmospheric obstacle and subsequent formation of an induced magnetosphere.

For planets orbiting fast-rotating stars, the joint evolution of both XUV-exposed atmospheres and stellar winds results in significant atmospheric confinement (10 planetary radii) at early ages around 50 Myr. The planetary atmosphere becomes less confined from 150 Myr, reaching a maximum extension of more than 25 planetary radii at 300 Myr, even though part of the atmosphere has been lost by means of hydrodynamic thermal escape. From 300 Myr, as a consequence of massive photoevaporation of the planetary atmosphere, resulting in higher confinement by the stellar wind, the atmosphere is reduced to 15.8 R_p.

For Earth-like planets orbiting slow-rotating stars, no significant changes have been reported in the 50-500 Myr period. This period is characterized by moderate and stable stellar activity, where planetary atmospheres remain almost unchanged, experiencing only minor mass-losses. Atmospheres during this time span extend up to 20 planetary radii, with a slightly reduced extension after 300 Myr, yet without significant changes in their distribution.

Our simulations reveal that the evolution in the extension of these escaping atmospheres is governed by the ram (dynamic) pressure balance between both stellar and planetary wind plasmas: in the case of planets orbiting rapidly rotating stars, there are more pronounced changes in the dynamic pressure of both plasmas. This is due to the rapid decrease in the parameters of the stellar wind and the rapid photoevaporation of the atmosphere caused by XUV radiation. In contrast, for planets around slowly rotating stars, no significant changes occur in the ram pressure of the stellar and planetary winds, resulting in stable atmospheres.

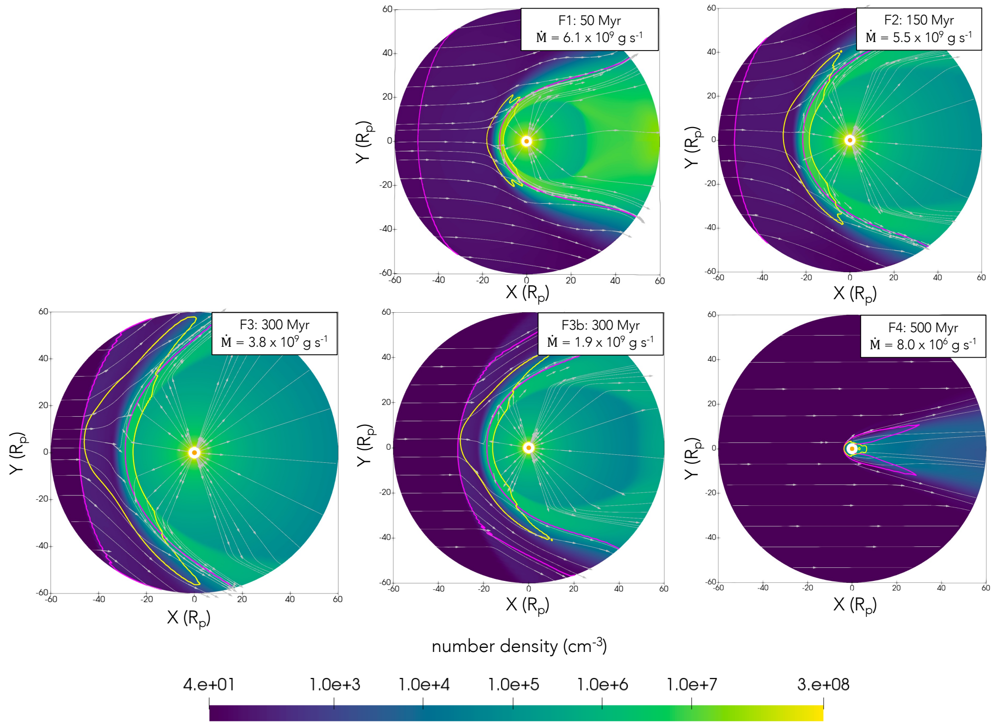

Figure 1: Density distribution map in the ecliptic plane for an Earth-like planet orbiting a fast-rotating star in the age range from 50 to 500 Myr. Grey thin lines represent the flow stream lines. Pink and yellow thick lines are for alfvénic and sonic surfaces, respectively.

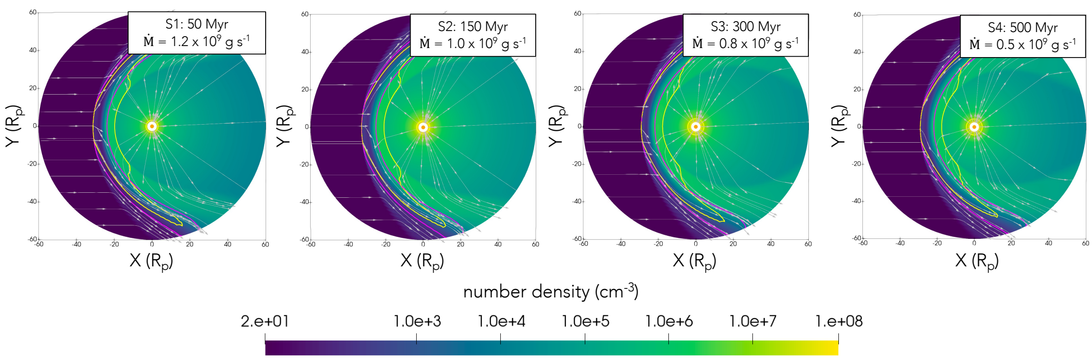

Figure 2: Same as Fig. 1, but considering models in the stellar slow-rotating regime.

Our simulations allow us to measure the atmospheric erosion caused by the isolated effect of stellar winds. These winds contribute an additional 1-4% to the loss triggered by XUV radiation for planets orbiting rapidly and slowly rotating stars, within the range of 50 to 500 Myrs.

Moreover, we compared the MHD interaction performed in this work with the HD interaction, keeping the same values for atmospheric and stellar wind ram pressures but neglecting the presence of magnetic fields. Incorporating magnetic fields into the stellar wind-planet interaction leads to further confinement of the planetary atmosphere due to the added magnetic pressure. This accentuates the significance of acknowledging the substantial role of magnetic fields in these interactions, and the limitations of studying stellar wind-planet interactions under the hydrodynamic approach.

In summary, this study highlights the extent to which stellar wind interaction cannot be disregarded in the early evolution of primordial planetary atmospheres, as it stands as a pivotal factor shaping the morphology of these gaseous envelopes and their detectability. Nevertheless, accounting for the mass-loss rates induced by the action of stellar winds, we can conclude that the overall losses of these atmospheres remain primarily governed by the influence of the star's photoevaporative radiation.

Acknowledgements

This work has been partially financed by the Ministry of Science and Innovation through grants: ESP2017-87813-R and PID2020-116726RB-I00, US DOE under grant DE-FG02-04ER54742 and the project 2019-T1/AMB-13648 funded by the Comunidad de Madrid.

References

[1] Canet, A. & Gómez de Castro, A. I. 2023, MNRAS, 525, 286. doi:10.1093/mnras/stad2148

[2] Carolan, S., Vidotto, A. A., Hazra, G., et al. 2021, MNRAS, 508, 6001. doi:10.1093/mnras/stab2947

[3] Erkaev, N. V., Lammer, H., Odert, P., et al. 2013, Astrobiology, 13, 1011. doi:10.1089/ast.2012.0957

[4] Johnstone, C. P., Güdel, M., Brott, I., et al. 2015, A&A, 577, A28. doi:10.1051/0004-6361/201425301

[5] Johnstone, C. P., Güdel, M., Stökl, A., et al. 2015, ApJL, 815, L12. doi:10.1088/2041-8205/815/1/L12

[6] Lammer, H., Stökl, A., Erkaev, N. V., et al. 2014, MNRAS, 439, 3225. doi:10.1093/mnras/stu085

[7] Matsakos, T., Uribe, A., & Königl, A. 2015, A&A, 578, A6. doi:10.1051/0004-6361/201425593

[8] McCann, J., Murray-Clay, R. A., Kratter, K., et al. 2019, ApJ, 873, 89. doi:10.3847/1538-4357/ab05b8

[9] Mignone, A., Bodo, G., Massaglia, S., et al. 2007, ApJS, 170, 228. doi:10.1086/513316

[10] Tu, L., Johnstone, C. P., Güdel, M., et al. 2015, A&A, 577, L3. doi:10.1051/0004-6361/201526146

[11] Vidotto, A. A., Gregory, S. G., Jardine, M., et al. 2014, MNRAS, 441, 2361. doi:10.1093/mnras/stu728

[12] Weber, E. J. & Davis, L. 1967, ApJ, 148, 217. doi:10.1086/149138